RNA BIOLOGY
2024, VOL. 21, NO. 1, 11–22
https://doi.org/10.1080/15476286.2024.2392304

Taylor & Francis
Taylor & Francis Group

RESEARCH PAPER

OPEN ACCESS Check for updates

FMRP cooperates with miRISC components to repress translation and regulate neurite morphogenesis in *Drosophila*

Navneeta Kaul[a], Sarala J. Pradhan[a], Nathan G. Boin[a], Madeleine M. Mason[a], Julian Rosales[b], Emily L. Starke[a], Emily C. Wilkinson[a], Erich G. Chapman[a,b,c], and Scott A. Barbee[a,c]

[a]Department of Biological Sciences, University of Denver, Denver, CO, USA; [b]Department of Chemistry and Biochemistry, University of Denver, Denver, CO, USA; [c]Molecular and Cellular Biophysics Program, University of Denver, Denver, CO, USA

ABSTRACT

Fragile X Syndrome (FXS) is the most common inherited form of intellectual disability and is caused by mutations in the gene encoding the Fragile X messenger ribonucleoprotein (FMRP). FMRP is an evolutionarily conserved and neuronally enriched RNA-binding protein (RBP) with functions in RNA editing, RNA transport, and protein translation. Specific target RNAs play critical roles in neurodevelopment, including the regulation of neurite morphogenesis, synaptic plasticity, and cognitive function. The different biological functions of FMRP are modulated by its cooperative interaction with distinct sets of neuronal RNA and protein-binding partners. Here, we focus on interactions between FMRP and components of the microRNA (miRNA) pathway. Using the *Drosophila* S2 cell model system, we show that the *Drosophila* ortholog of FMRP (dFMRP) can repress translation when directly tethered to a reporter mRNA. This repression requires the activity of AGO1, GW182, and MOV10/Armitage, conserved proteins associated with the miRNA-containing RNA-induced silencing complex (miRISC). Additionally, we find that untagged dFMRP can interact with a short stem-loop sequence in the translational reporter, a prerequisite for repression by exogenous miR-958. Finally, we demonstrate that dFmr1 interacts genetically with GW182 to control neurite morphogenesis. These data suggest that dFMRP may recruit the miRISC to nearby miRNA binding sites and repress translation via its cooperative interactions with evolutionarily conserved components of the miRNA pathway.

ARTICLE HISTORY
Revised 29 July 2024
Accepted 6 August 2024

KEYWORDS
Drosophila; FXS; FMRP; RNA-binding proteins; miRNA pathway

Introduction

Fragile X Syndrome (FXS) is the most common inherited neurodevelopmental disorder in humans and the leading monogenetic cause of autism [1]. Most cases of FXS are caused by the expansion of the CGG trinucleotide repeat (>200) in the 5' untranslated region (UTR) of the X-linked *FMR1* gene, which leads to DNA hypermethylation and epigenetic transcriptional silencing. *FMR1* encodes the Fragile X messenger ribonucleoprotein (FMRP), a conserved RNA-binding protein (RBP) implicated in multiple steps of RNA metabolism, including RNA editing, translation, and transport [2,3]. FMRP contains canonical RNA-binding motifs, including two heterogeneous nuclear ribonucleoprotein K homology (KH) domains and an arginine-glycine-glycine (RGG) motif [2]. Numerous studies have shown that FMRP binds to thousands of mRNAs in the brain, many of which regulate processes such as neurite morphogenesis and synaptic plasticity [4].

FMRP is best characterized as a repressor of translation, and the loss of translational control is widely believed to be linked to the deficits seen in FXS [5]. FMRP represses translation via several distinct mechanisms. First, mammalian FMRP can repress cap-dependent translation in specific target mRNAs by interacting with the Cytoplasmic FMRP Interacting Protein (CYFIP) [6]. Second, FMRP is well-characterized as a repressor of translational elongation. FMRP co-sediments with polyribosomes in sucrose gradients, suggesting it may cause the reversible stalling of ribosomes on target mRNAs [7]. In humans, FMRP can inhibit elongation in vitro via its RGG motif and intrinsically disordered C-terminal domain [8]. In contrast, cryo-EM studies in *Drosophila* have revealed that the KH1 and KH2 domains of fly FMRP can directly interact with the ribosomal L5 protein on the 80S ribosome to block translation elongation [9].

FMRP also represses the translation of specific target mRNAs by interacting with conserved components of the microRNA (miRNA) pathway [10]. First, mammalian FMRP can reversibly interact with the riboendonuclease, Dicer, and is thought to modulate the processing of precursor miRNAs (pre-miRNAs) into mature miRNAs [11]. Second, both mammalian and *Drosophila* FMRP biochemically interact with the Argonaute (AGO) proteins, core components of the RNA-induced silencing complex (RISC) [12,13]. AGO proteins function to bind small noncoding RNAs (such as miRNAs

CONTACT Scott A. Barbee scott.barbee@du.edu Department of Biological Sciences, University of Denver, 2101 E. Wesley Ave., Denver, CO 80210, USA
Supplemental data for this article can be accessed online at https://doi.org/10.1080/15476286.2024.2392304

© 2024 The Author(s). Published by Informa UK Limited, trading as Taylor & Francis Group.
This is an Open Access article distributed under the terms of the Creative Commons Attribution-NonCommercial License (http://creativecommons.org/licenses/by-nc/4.0/), which permits unrestricted non-commercial use, distribution, and reproduction in any medium, provided the original work is properly cited. The terms on which this article has been published allow the posting of the Accepted Manuscript in a repository by the author(s) or with their consent.

and siRNAs) and facilitate their interaction with specific sequences in target mRNAs. Finally, mammalian FMRP binds directly to the RISC-associated RNA helicase, MOV10 [14]. Interestingly, the FMRP/MOV10 complex has been shown to both block and activate the translation of distinct target mRNAs by reversibly modulating the ability of the miRNA-containing RISC (miRISC) to bind to nearby target sequences [10,15].

A critical outstanding question in the field is understanding how FMRP represses the translation of bound mRNAs by recruiting components of the miRNA pathway. The AGO proteins alone are insufficient to mediate the miRNA-mediated silencing of target mRNAs [16]. Instead, silencing is facilitated by the AGO-associated GW182 proteins. GW182 is an effector in the miRISC and acts as a scaffold to recruit proteins required for translational repression or mRNA deadenylation, followed by 5'-to-3' exonucleolytic decay [16]. In this study, we have developed a novel functional assay to better understand how the *Drosophila* ortholog of FMRP (dFMRP) represses translation via the miRNA pathway. We found that dFMRP can repress translation when directly tethered to a luciferase reporter mRNA in *Drosophila* S2 cells. Repression of the reporter is abrogated by the depletion of miRNA pathway components through RNA interference (RNAi). Finally, we show that *dFmr1* interacts genetically with GW182 to regulate synapse morphogenesis *in vivo*. Taken together, our findings support a model where FMRP binding may act as a tether to recruit the miRISC to nearby miRNA binding sites to facilitate translational repression via the miRNA pathway. Moreover, based on our findings, we propose that this FMRP tethering assay can be used as a tool to rapidly screen novel FMRP-interacting proteins to determine if they interact cooperatively to regulate translation of reporter mRNAs.

Results

dFMRP can repress reporter translation in a tethered functional assay

To better understand how dFMRP regulates translation, we adapted a functional tethering assay to study dFMRP activity in *Drosophila* Schneider (S2) cells [17]. Full-length dFMRP was fused to an N-terminal λN-HA tag and co-expressed with a firefly luciferase (FLuc) reporter containing five tandem λN binding sites (BoxB hairpins) (Figure 1A). These were co-expressed with a Renilla luciferase (RLuc) reporter as a transfection control. S2 cells were transfected with increasing concentrations of tagged dFMRP or a λN-HA control (Figure 1B). As expected, the expression of full-length dFMRP significantly repressed reporter expression at all concentrations tested (Figure 1C) [17]. This repression occurred at the level of translation and not mRNA decay because the amount of polyadenylated mRNA did not similarly decrease (Figure 1C).

To further understand how dFMRP represses translation mechanistically, we assessed the translation status of the reporter mRNA using polysome profiling in cells transfected with 0.5 µg of the plasmid expressing dFMRP or the control (Supplemental Figure S1). We found a notable redistribution of reporter mRNA to light polysome fractions after the expression of dFMRP (Figure 1D), indicating a shift in the distribution rather than a change in the total mRNA level (Figure 1C). The reduction in 40S, 60S, and the loss of monosomes is consistent with a block at the level of translational initiation. This finding aligns with previous work showing that GW182 represses translation at the initiation step in *Drosophila*, *C. elegans*, and human cells [18–20].

Next, we analysed the ability of dFMRP to repress translation using two additional reporters (Figure 1A). The first reporter contained a 3' end generated by a self-cleaving hammerhead ribozyme (HhR) that lacks a poly(A) tail and consequently cannot be targeted for deadenylation [20]. The second reporter lacked a poly(A) tail but contained a short 5' UTR (8 nucleotides) which can initiate translation without ribosome scanning [21]. Full-length dFMRP was capable of similarly repressing all reporters, reducing translation to ~40% of λN-HA controls (Figure 1E). These data suggest that tethered dFMRP can repress reporter translation via a ribosome scanning- and deadenylation-independent mechanism.

Finally, to dissect the functional domains of dFMRP involved in translational repression, we conducted experiments using various deletion constructs of dFMRP. These constructs included deletions of the KH0 domain, KH1 and KH2 domains, and the RGG domain (Figure 1F). These functional domains and deletions in dFMRP are identical to those previously described [17,22,23]. We then tethered these constructs to the polyadenylated BoxB reporter (Figure 1G). Our observations revealed that the deletion of the RGG domain had no effect on repression, indicating that this domain is not crucial for the translational repression activity of dFMRP. However, we cannot rule out that this result is simply an artefact of the tethered repression assay. In contrast, the deletion of the KH1 and KH2 domains resulted in significant derepression of translation, highlighting their essential role in this process. Furthermore, the deletion of the KH0 domain failed to repress translation, but this effect was significant only at high concentrations. Collectively, these results underscore the importance of the KH1 and KH2 domains in dFMRP-mediated translational repression and are consistent with our published work showing that FXS-causing missense mutations in the KH1 and KH2 domains disrupt their function in translation [17].

dFMRP represses reporter translation via conserved components of the miRNA pathway

The *Drosophila* miRNA proteins AGO1 and GW182 have been shown to regulate all three FLuc reporters in a manner similar to dFMRP (Figure 1A) [21]. To verify this, we obtained and tested plasmids expressing λN-HA tagged full-length AGO1 and GW182 in the tethering assay. As expected, both AGO1 and GW182 significantly repressed translation of the reporter, with results more robust than those for dFMRP (Figure 1E). Given the well-established genetic and biochemical interaction between FMRP and the miRNA pathway [24], we next investigated whether repression of the reporter required additional components of the miRNA pathway.

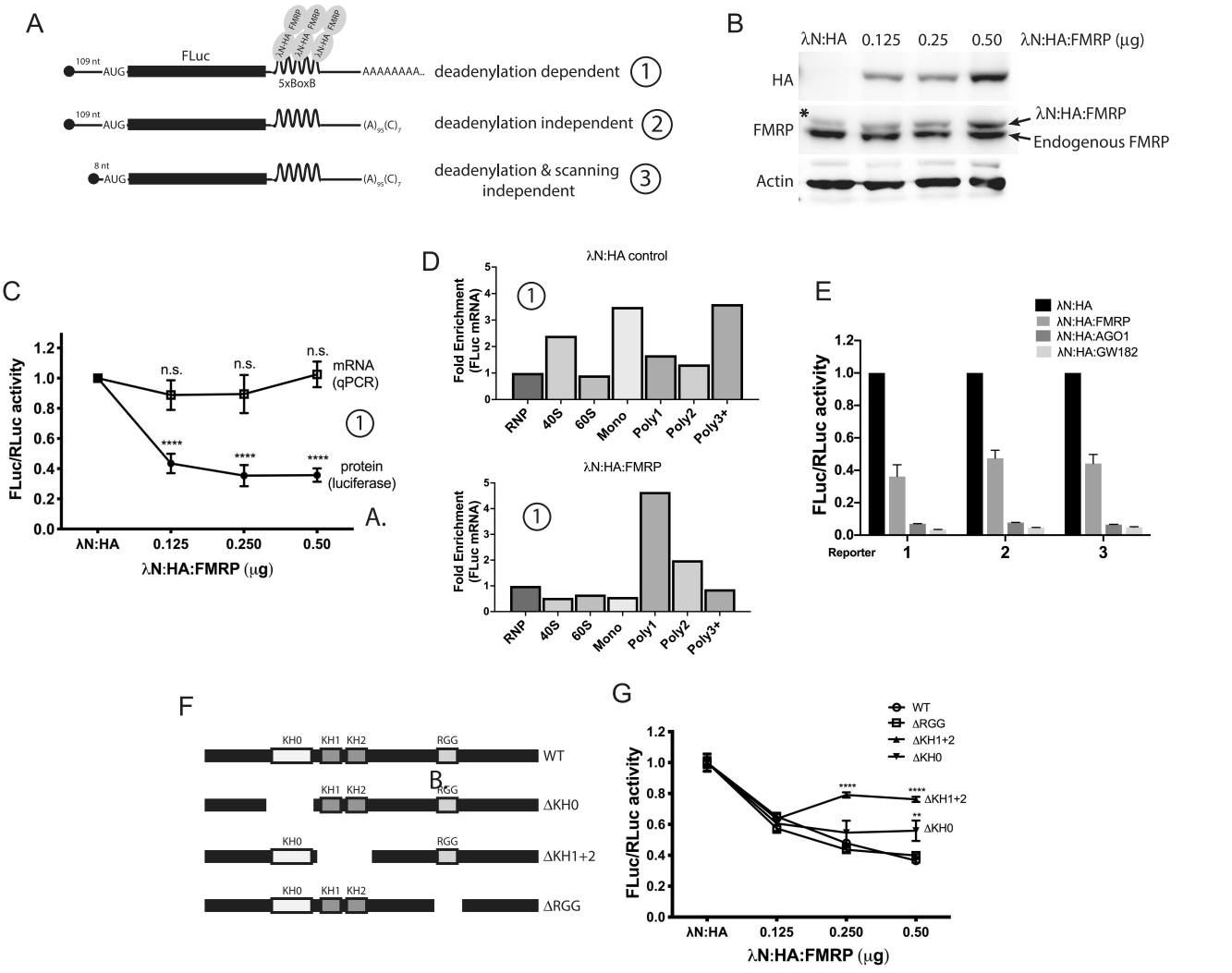

Figure 1. FMRP silences translation of reporter mRNAs via a deadenylation- and scanning- independent mechanism. (A) Schematic representation of the translational reporters used in figure 1 and 2. (B and C) tethering assay in S2 cells transfected with FLuc-5×BoxB reporter #1 and increasing concentrations of a plasmid expressing λN-HA tagged dFMRP. (B) Western blot showing levels of λN-HA-dFMRP relative to endogenous FMRP and an Actin loading control. (C) FLuc activity and RNA levels were normalized to those of the RLuc transfection control and then shown relative to the λN-HA peptide negative control after its values were set to 100%. The asterisk marks a band in the control corresponding to a heavier isoform of endogenous dFMRP. (D) FLuc reporter #1 RNA abundance in fractions collected for polysome profiling. Relative fold enrichment was calculated relative to RNA levels in the small RNP fraction for each condition. (E) FLuc activity of the indicated reporters after tethering FMRP, AGO1, and GW182. Results for each reporter were normalized and described for (C). All luciferase assay and qPCR experiments were done in three biological replicates. Statistical significance for results in (C) was determined by one-way ANOVA followed by a Dunnett's multiple comparison test. Statistical significance for results in (G) was determined by two-way AVOVA followed by a Dunnett's multiple comparison test. ** $p < 0.01$, **** $p < 0.0001$. Error bars represent the mean ± standard error (SE).

We initially focused on GW182 because it is the effector in the miRISC and directly induces translational repression, whereas AGO1 alone is insufficient for silencing [16]. To examine this interaction, we co-transfected S2 cells with λN-HA tagged dFMRP, FLuc and RLuc reporters and double-stranded RNA (dsRNA) targeting two regions of the GW182 transcript. Knockdown of GW182 expression with both dsRNAs led to significant derepression of reporter translation by dFMRP (Figure 2A,B). To further explore this interaction, we expanded our analysis to include additional conserved components of the miRNA pathway that have been shown to interact with FMRP in both *Drosophila* and mammals. As with GW182, knockdown of Ago1 expression resulted in significant de-repression of reporter translation (Figure 2C,D). Similarly, knockdown of Dcr1 expression also resulted in statistically significant de-repression (Figure 2C,D). Additionally, knockdown of Armitage (the *Drosophila* ortholog of MOV10) led to significant de-repression of the reporter (Figure 2C,D). Lastly, co-transfection with dsRNA targeting GFP (not expressed in the S2 cell system) had no impact on translational repression by FMRP (Figure 2C). These data suggest that reporter repression by FMRP requires multiple components of the miRNA pathway. Unfortunately, published antibodies targeting Armitage did not work in our hands [25].

FMRP colocalizes strongly with AGO1-containing cytoplasmic granules

It is well described that FMRP associates with membraneless cytoplasmic granules that contain RNA-binding proteins (RBPs) and translationally repressed mRNAs [3]. Based on

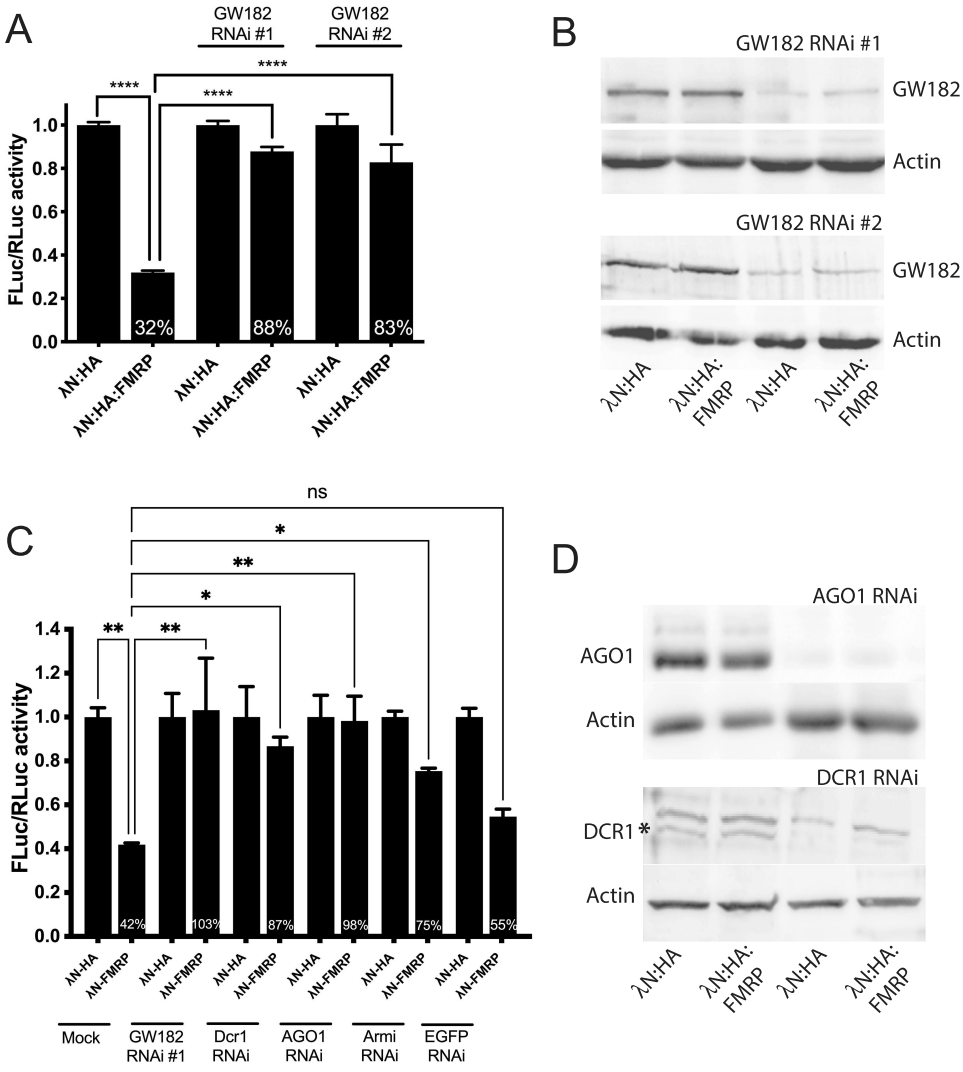

Figure 2. Reporter mRNA repression by tethered FMRP requires conserved components of the miRNA pathway. (A) FLuc activity in S2 cells transfected FLuc-5×BoxB reporter #1, λN-HA tagged dFMRP, and dsRNA targeting two non-overlapping regions of the *GW182* transcript. (B) Western blot showing levels of GW182 expression with and without co-transfected dsRNA. (C) FLuc activity in S2 cells transfected FLuc-5×BoxB reporter #1, λN-HA tagged dFMRP, and dsRNA targeting the mRNAs encoding for GW182, DCR1, AGO1, and EGFP (negative control). D) Western blot showing levels of AGO1 and DCR1 expression with and without co-transfected dsRNA. The asterisk marks the 255 kDa DCR1 protein. As there are no other predicted isoforms of DCR1 in *Drosophila*, and it is not affected by *Dcr1* RNAi, the higher band is likely nonspecific. All experiments shown were done in triplicate. Statistical significance for results in A and C was determined by one-way ANOVA followed by a Tukey's multiple comparison test. Significance between each of the specific conditions is indicated by brackets. *$p < 0.05$, ****$p < 0.0001$. Error bars represent the mean ± standard error (SE).

the requirement for the miRNA pathway to repress reporter translation, we hypothesized that, as seen with human orthologs, miRISC proteins may colocalize with dFMRP in these granules [13]. To test this, we co-transfected S2 cells with a plasmid expressing a GFP-tagged full-length dFMRP protein along with one expressing mCherry-tagged miRNA pathway proteins (Figure 3A). As expected, dFMRP colocalized very strongly with AGO1 in S2 cells (Figure 3A,B). In contrast, while we observed dFMRP granules without GW182 and Dcr1, we also noted instances where AGO1- and GW182-containing granules colocalized with dFMRP (Figure 3C).

It has also been shown that dFMRP interacts biochemically with AGO1, although its association with GW182 has not been investigated [12]. Moreover, the dependence of this association on RNA is not known. To address these questions, we co-transfected S2 cells with plasmids expressing λN-HA-tagged dFMRP and either FLAG-tagged AGO1 or GW182. Consistent with published results, AGO1 co-immunoprecipitated strongly with dFMRP, but we found that this interaction is not dependent on RNA (Figure 3D) [12,13]. Similarly, we show that GW182 also interacted with dFMRP in an RNA-independent manner (Figure 3D). This result is not unexpected as human GW182 binds directly to AGOs within the miRISC, and GW182 subsequently acts as a bridge between AGOs and downstream effectors [26,27]. Taken together, these data suggest that there is a protein–protein interaction between dFMRP and the miRISC.

dFMRP can interact with the BoxB hairpin sequence and repress reporter translation

Mouse and human FMRP have been shown to bind several sequence and structural elements in target transcripts via their RNA-binding domains. These motifs include G-quadruplexes

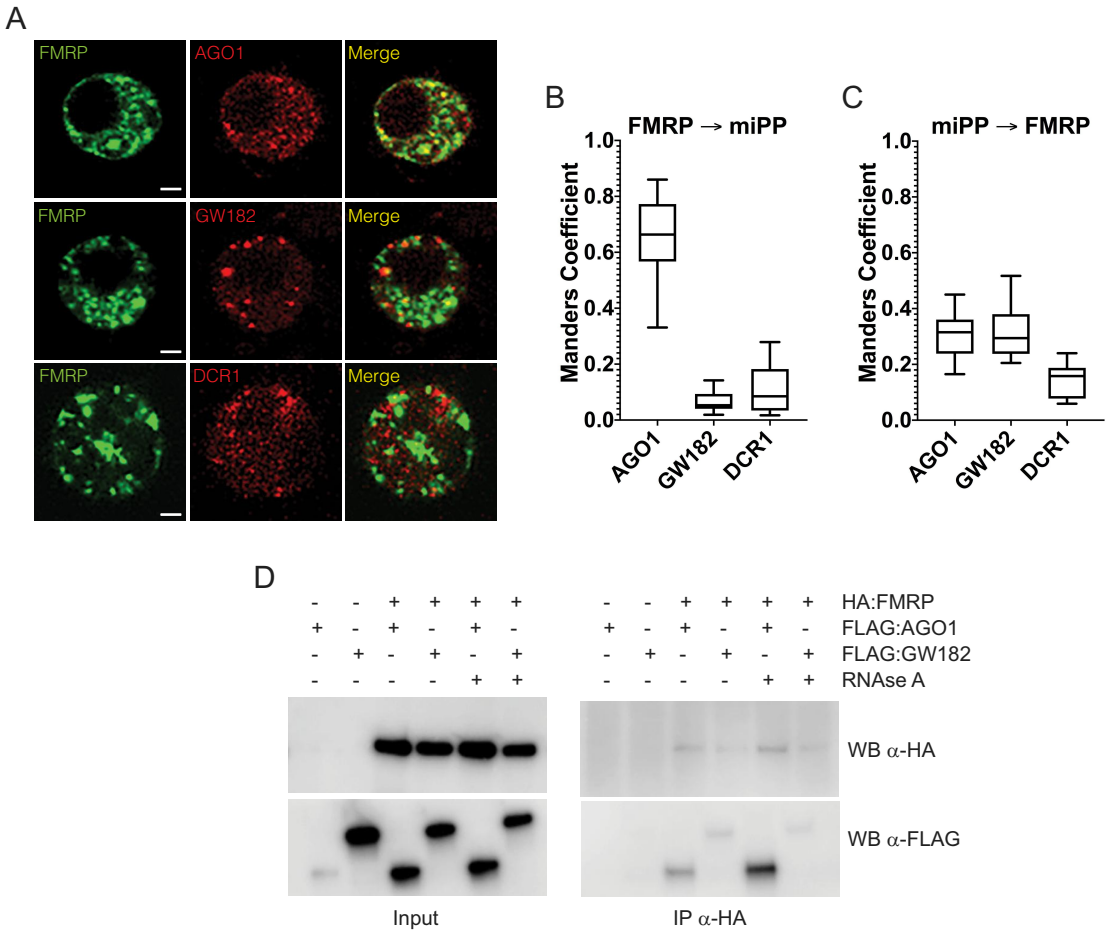

Figure 3. FMRP colocalizes and biochemically interacts with component of the miRISC. (A) Confocal micrographs of representative S2 cells transfected with tagged dFMRP (green) and the indicated mCherry-tagged miRNA pathway protein (miPP; red). Merged images are included for visual comparison of the colocalization (or lack of colocalization) between proteins. Scale bars = 2 µm. (B and C) graphs showing the degree of overlap as determined by Manders correlation coefficients between green FMRP pixels that also contain red miPP fluorescence (B) and *vice versa* (C). Number of cells analyzed for colocalization were: FMRP/AGO1 ($n = 12$), FMRP/GW182 ($n = 14$), and FMRP/DCR1 ($n = 13$). (D) Western blots showing results of co-immunoprecipitation assays in S2 cells cotransfected with λN-HA tagged dFMRP and FLAG-tagged AGO1 or GW182. To determine if RNA is required to facilitate interactions between proteins, some reactions were incubated with RNAse a during the immunoprecipitation step.

via the RGG box domain [28]. Additionally, the KH domains have been shown to interact with an RNA pseudoknot structure and two short sequences that are enriched in FMRP-bound transcripts, WGGA and ACUK (where K = G/U and W = A/U) [29,30]. Interestingly, FMRP has also been shown to bind to a structural element consisting of three tandem stem loops in the *Sod1* mRNA and regulate its translation [31]. Based on this, we hypothesized that dFMRP may be able to bind directly to the BoxB stem loop within the 3'UTR of the reporter transcript.

To test this, we conducted an electrophoretic mobility shift assay (EMSA) using purified full-length dFMRP protein and a minimal RNA probe consisting of a single BoxB stem loop sequence (Figure 4A). We observed that at least some of the BoxB RNA shifted upward in a concentration-dependent manner, unlike the A14 control RNA, indicating that the shift is specific to the BoxB sequence (Figure 4B). However, we acknowledge that FMRP is likely to form aggregates (or phase separate) at higher concentrations, which may cause the protein to get stuck in the well, resulting in not all the probe shifting [32]. This experiment was conducted to address the observation that the untagged dFMRP construct, which we initially assumed would serve as a control, was also capable of reporter repression. Together, these data confirm that untethered dFMRP does have some affinity for the minimal BoxB stem loop sequence.

Next, we asked if dFMRP could repress the expression of the luciferase reporter containing five tandem BoxB sequences (5×BoxB). We co-transfected S2 cells with the reporter and increasing concentrations of a plasmid expressing dFMRP lacking the λN-HA tagged tag. We observed that untethered FMRP was able to significantly repress reporter expression, even at the lowest concentrations tested (Figure 4D). To examine this interaction further, we constructed a series of reporters that contained three, one, or no tandem BoxB stem loops (3×BoxB, 1×BoxB, and 0×BoxB) and similarly co-transfected S2 cells with increasing concentrations of dFMRP (Figure 4C). dFMRP was able to repress translation of the 1×BoxB reporter as efficiently as it did the 5×BoxB reporter (Figure 4D). In comparison, removal of all BoxB stem loops abolished the ability of dFMRP to repress expression (Figure 4D). Together, this suggests that endogenous dFMRP can repress translation of the reporter by interacting with the BoxB sequence.

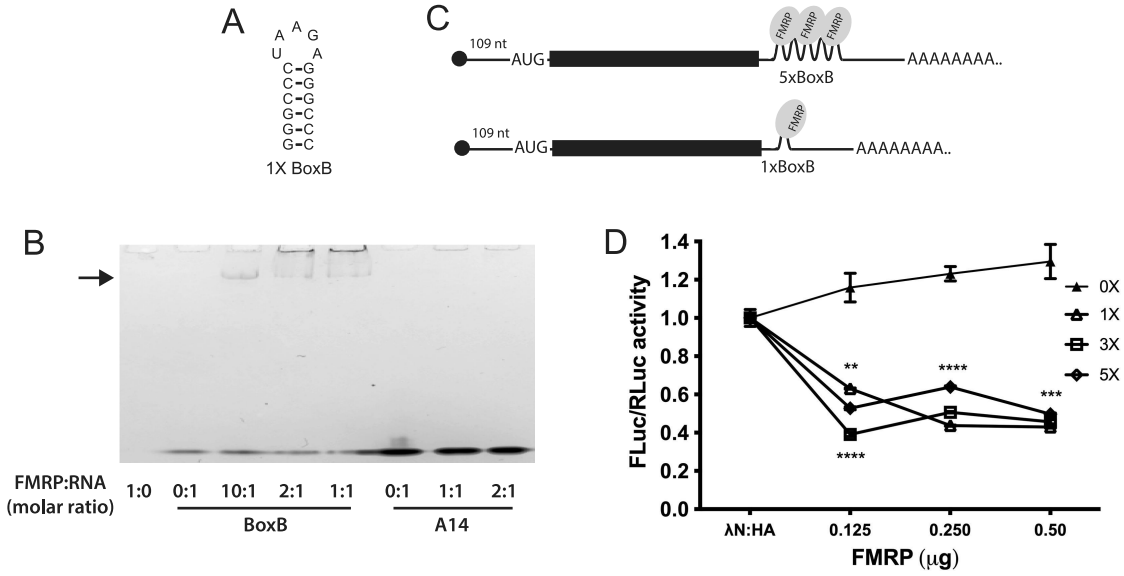

Figure 4. Untagged and untethered FMRP can bind directly to the BoxB stem loop to repress reporter translation. (A) The predicted structure of the 1×BoxB stem loop. (B) A 'cold' native gel showing results of the EMSA experiments. Purified dFMRP was incubated with *in vitro* transcribed RNAs corresponding to the minimal 1×BoxB stem loop or an A14 unstructured control at the indicated molar ratio. The bands and the bottom of the gel show the unbound RNA probes. The arrow indicates supershifted 1×BoxB probe bound to dFMRP. (C) Schematic representation of two translational reporters used in Figure 4D. (D) Luciferase assay in S2 cells transfected with the indicated FLuc-BoxB reporters and increasing concentrations of a plasmid expressing untagged dFMRP. Statistical significance was determined by two-way ANOVA followed by a Dunnett's multiple comparison test. $^{**}p < 0.01$, $^{***}p < 0.001$, $^{****}p < 0.0001$. Error bars represent the mean ± standard error (SE).

Repression of reporter translation by miR-958 requires FMRP and the BoxB motif

The discovery that dFMRP can interact with and repress the reporter led us to investigate whether repression via the miRNA pathway also requires dFMRP. We first used a bioinformatic approach to identify putative miRNA binding sites within the 3'UTR of the reporter and found a strong predicted binding site for miR-958 located ~60 nucleotides downstream of the 1×BoxB stem loop (Figure 5A; seed = 7mer-m8, $\Delta\Delta G = -12.7$). This miR-958 binding site is present in all translation reporters used in this study as they share a common 3'UTR. We have shown that miR-958 regulates rapid activity-dependent neurite growth at the *Drosophila* larval neuromuscular junction (NMJ) suggesting it may be biologically relevant to FXS phenotypes [33]. It is important to note that miR-958 is not expressed in the S2 cell variant used in our experiments.

To address whether the 1×BoxB reporter is a target for repression by miR-958, we co-transfected S2 cells with the 1×BoxB reporter and a plasmid expressing the primary miRNA (pri-miRNA) sequence encoding miR-958, as we have done previously *in vivo* [33]. We found that reporter expression was significantly reduced (Figure 5B). Next, to determine if repression by miR-958 required dFMRP activity, we co-transfected cells with the 1×BoxB reporter, miR-958, and dsRNA targeting the dFmr1 transcript. Knockdown of *dFmr1* expression completely disrupted the ability of miR-958 to repress reporter expression (Figure 5B,C). To confirm this result, we examined whether miR-958 could repress translation of the 0×BoxB reporter, which retains the predicted miR-958 binding site but lacks the BoxB stem-loop sequence (Figure 5A). Similar to *dFmr1* knockdown, removal of the BoxB stem loop abolished the repression activity of miR-958 (Figure 5B). Collectively, these data strongly suggest that the translational repression activity of miR-958 first requires dFMRP interaction with the BoxB sequence. However, the specific miRNA in S2 cells involved in AGO1/GW182-mediated repression has not yet been identified.

dFmr1 interacts genetically with GW182 to regulate neurite morphogenesis at the NMJ

Loss of *dFmr1* expression causes significant defects in synapse structure and function at the Drosophila larval NMJ [34]. Additionally, *dFmr1* interacts genetically with *Ago1* to regulate synaptic growth and structure at the NMJ [12]. Specifically, larvae heterozygous for both *dFmr1* and *Ago1* exhibit overgrowth and overelaboration of synaptic terminals, a phenotype similar to that seen with *dFmr1* loss-of-function [12]. Both AGO1 and GW182 are co-expressed with FMRP in motor neuron cell bodies in the larval CNS (Supplemental Figure S2). Based on these observations, we sought to determine if *dFmr1* similarly interacted genetically with *GW182* to regulate NMJ morphogenesis. The *Drosophila* larval NMJ is used as a genetic model for the study of glutamatergic synapses in the mammalian brain [35]. One of its notable properties is that its terminal synaptic boutons exhibit a high degree of plasticity during development [36]. For this analysis, we examined the NMJs innervating muscle 6/7 in abdominal segment 3 of third instar larvae. This NMJ contains two types of glutamatergic boutons: 1b (big) and 1s (small), derived from two distinct neurons [37]. Type 1b boutons are highly plastic and can be distinguished by their larger size and higher levels of the postsynaptic density marker, Dlg [38].

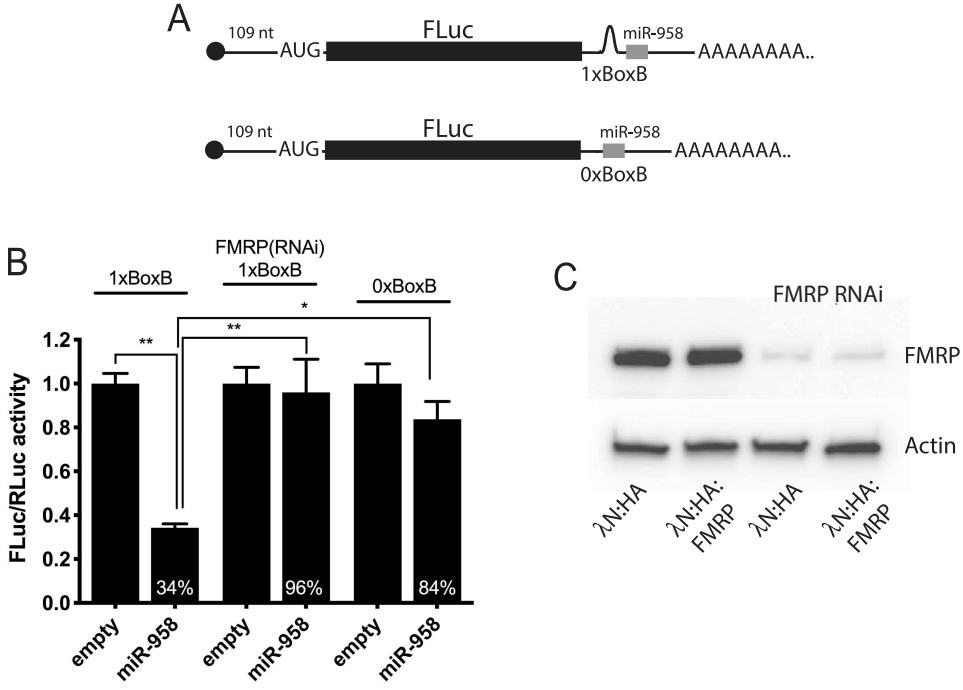

Figure 5. Reporter mRNA repression by miR-958 requires FMRP and the BoxB stem loop. A) schematic representation of the translational reporters used in Figure 5 with the predicted binding site for miR-958. (B) FLuc activity in S2 cells transfected with the indicated FLuc-BoxB reporter (0×BoxB or 1×BoxB), a plasmid expressing the primary miR-958 (or an empty vector control), and (as indicated) dsRNA targeting the mRNA encoding for dFMRP. (C) Western blot showing levels of dFMRP expression with and without co-transfected dsRNA. Statistical significance was determined by one-way ANOVA followed by a Tukey's multiple comparison test. Significance between specific conditions is indicated by brackets. *$p < 0.05$, **$p < 0.01$. Error bars represent the mean ± standard error (SE).

To determine if *dFmr1* and *GW182* interact to regulate NMJ morphogenesis, we analysed double heterozygotes (*dFmr1 -/+; GW182 -/+*) and compared the results to single heterozygotes and a control for genetic background (Figure 6). Synapse size was quantified by counting the number of type 1b synaptic boutons. We observed a statistically significant increase in synaptic bouton number in *dFmr1 -/+; GW182 -/+* larvae relative to controls (Figure 6F,G). This was seen despite the *GW182 -/+* single heterozygote having a strong overgrowth phenotype (Figure 6D,G). As a positive control, we examined the genetic interaction between *dFmr1* and *Ago1*. Surprisingly, we observed a significant, but much weaker, overgrowth phenotype than expected (Figure 6E,G). Differences between our results and those reported by Jin et al. [12] are likely due to differences in dFmr1 alleles and normalization methods. Taken together, these data support

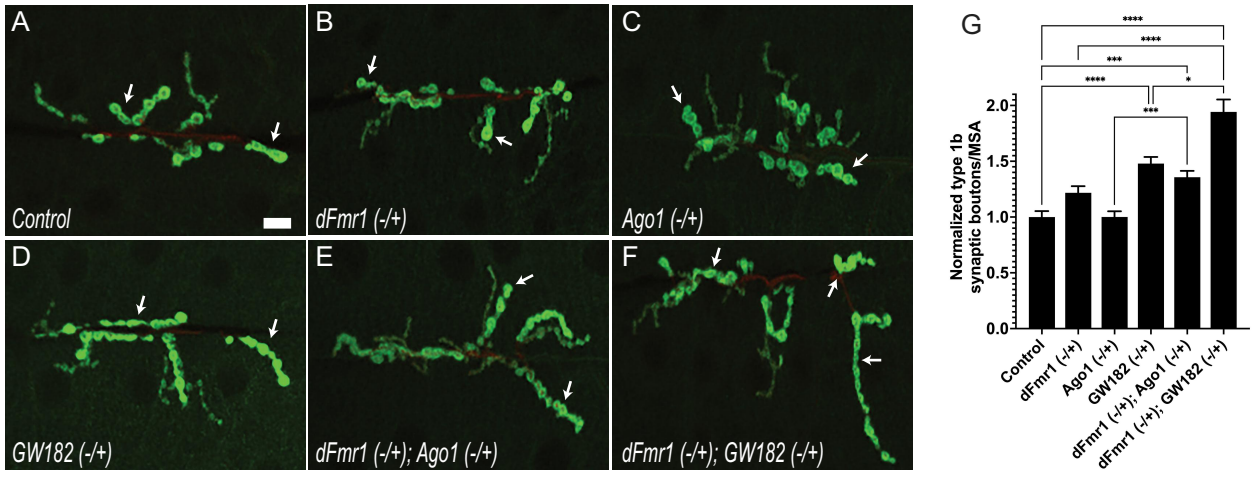

Figure 6. *dFmr1* interacts genetically with *GW182* to regulate neurite morphogenesis and the larval NMJ. (A-F) Representative images from the indicated genotypes of third instar larval NMJs immunostained with antibodies targeting DLG (green). Larger type 1b boutons are indicated by arrows. Scale bar = 10 µm. (G) The average number of type 1b synaptic boutons per NMJ for each genotype normalized to MSA. Values are shown relative to the w^{1118} *(Iso31)* negative control after its values were set to 100%. Statistical significance was determined using a brown-forsyth and Welch ANOVA followed by a Dunnett's multiple comparison test. Significance between specific genotypes is indicated by brackets. *$p < 0.05$, ***$p < 0.001$, ****$p < 0.0001$. Error bars represent the mean ± standard error (SE).

a model where *dFmr1* requires multiple components of the miRISC to regulate the normal development of glutamatergic synapses in the *Drosophila* model system.

Discussion

One critical function of FMRP is to regulate the translation of specific target mRNAs by blocking translational initiation, elongation, or acting through the miRNA pathway. However, what determines which of these mechanisms FMRP will utilize? Three lines of evidence suggest that this depends on combinatorial interactions with specific protein-binding partners and/or sequence elements within target mRNAs. First, FMRP can interact directly with CYFIP to regulate translational initiation [39]. This study shows that FMRP can recruit CYFIP to specific mRNAs, which sequesters the cap-binding protein eIF4E and thereby prevents initiation in cap-dependent translation. However, it is not clear which sequences are bound by FMRP in target mRNAs to facilitate this process. Second, FMRP can interact directly with the ribosome to inhibit translation elongation. CLIP-seq experiments have shown that mammalian FMRP binds primarily to short sequence elements in coding sequences via its KH domains [40]. Evidence suggests that dFMRP may directly block ribosome translocation by inhibiting the interaction of tRNAs or elongation factors [9]. Finally, an FMRP/MOV10 complex can bind to G-quadruplex sequences found in the 3'UTR of some target mRNAs. Interestingly, the FMRP/MOV10 interaction can protect a subset of bound mRNAs from AGO association, increasing levels of target mRNA expression [15]. In this case, the miRNA response element (MRE) is embedded within the G-quadruplex sequence, and MOV10 stabilizes the FMRP/quadruplex interaction via an unknown mechanism.

Our data support a model for translational repression by dFMRP via the miRNA pathway, where dFMRP/AGO1/GW182/Armitage complexes are directly recruited to specific sequence motifs located in the 3'UTR of target mRNAs. These sequence motifs include both a binding site for dFMRP and a nearby MRE recognized by a specific miRNA. Importantly, we predict that the MRE is accessible and not embedded in G-quadruplex, although we cannot rule out that it is masked by complex secondary structure. MOV10/Armitage, a helicase associated with the miRISC, plays a crucial role in this process by facilitating the unwinding of miRNA duplexes and aiding in the assembly of the active RISC. This allows for efficient targeting and binding of the miRNA to the MRE. Once the miRNA is loaded, GW182, the miRISC effector, along with Armitage, facilitates the translational repression of the target mRNA. Together, these components create a robust mechanism for dFMRP-mediated translational repression.

We provide evidence that a portion of cytoplasmic dFMRP colocalizes with AGO1 but not GW182 (Figure 3). This relationship is supported by co-immunoprecipitation data which suggests that dFMRP-containing complexes interact with AGO1 and GW182 (Figure 3D). Based on these data, we propose that dFMRP may be interacting with a pool of AGO1 that is not loaded with miRNAs. GW182 proteins have an increased affinity for AGOs after miRNA loading [26]. Our colocalization and co-immunoprecipitation data suggest that GW182 May be recruited to the miRISC once the AGO proteins are primed for target mRNA recognition. FMRP has also been shown to reversibly interact with Dicer-containing complexes [11]. After processing pre-miRNAs into mature miRNAs, Dicer transiently associates with AGOs while one strand is preferentially loaded [41]. Taken together, our data suggests that dFMRP is likely to be associated with AGO1 before, during, and after the biogenesis of the functional miRISC.

GW182 is an evolutionarily conserved core component of the miRISC in metazoans. It has been shown to interact directly with the AGO proteins and acts as a scaffold to aid in the recruitment of the CCR4-NOT deadenylase complex and, subsequently, the decapping enzymes [16]. Deadenylation followed by decapping triggers 5'-to-3' mRNA decay. Interestingly, our data suggests that dFMRP, AGO1, and GW182 can all repress translation of a reporter mRNA that cannot be deadenylated (Figure 1E). This is consistent with published results using tethered AGO1 and GW182 [21]. Moreover, dFMRP represses reporter translation with no changes in mRNA levels (Figure 1C). Taken together, these data suggest that dFMRP, AGO1, and GW182 May repress reporter translation via a deadenylation- and decay-independent mechanism. GW182 has also been shown to block translation, in the absence of mRNA decay, by interacting with poly(A)-binding proteins (PABPs) [16]. Mechanistically, the GW182/PABP interaction is thought to interfere with mRNA circularization and thereby reduce the efficiency of translational initiation [42,43]. Alternatively, the GW182/PABP interaction may reduce the affinity of PABP for the poly(A) tail. While we cannot rule out the idea that an FMRP/AGO1/GW182 complex is inhibiting elongation, our data suggest that it may instead be blocking initiation (Figure 1D).

Our data also shows that dFMRP is capable of interacting with the short BoxB sequence (Figure 4). Binding of FMRP to stem-loop structures in target RNAs is not unprecedented. First, human FMRP can bind directly to a short stem-loop in the noncoding Brain Cytoplasmic 1 (BC1) RNA [44]. Second, FMRP can bind directly to three tandem stem-loops in the mRNA encoding for mouse Superoxide Dismutase 1 (Sod1) and promote its translational activation [31]. Finally, mammalian FMRP has been shown to bind to more complex secondary structures in target RNAs, including G-quadruplexes through its RGG box and RNA pseudoknot structures (kissing complexes) through its KH2 domain [29,45,46]. Interestingly, while G-quadruplexes are the best characterized structural element bound by mammalian FMRP, data suggest that Drosophila FMRP does not bind with high affinity to the strong G-quadruplex structure found in the *sc1* RNA [47]. This study also determined that the RGG box in dFMRP is poorly conserved relative to its mammalian orthologs. Collectively, these data suggest that dFMRP may not bind to target RNAs through an RGG/G-quadruplex interaction. It is possible that the RGG box in dFMRP may have deviated in its binding affinity, perhaps for small stem-loop structures. Future work is needed to investigate if this mechanism is involved in the regulation of endogenous mRNAs.

Our study focuses on the role of dFMRP in translational repression via interactions at the 3'UTR of target mRNAs.

While our findings provide valuable insights into these specific interactions and highlight the contributions of dFMRP, AGO1, GW182 and MOV10/Armitage, they represent only a portion of FMRP's broader regulatory roles. FMRP is known to interact with various sequence and structural elements throughout entire mRNAs, influencing RNA transport, localization, and stability. The artificial reporter systems used in our study, while effective for dissecting specific interactions, may not fully capture the complexity of FMRP's functions in a native cellular context. Further studies are needed to explore FMRP's functions in other mRNA regions, such as the coding sequence and 5'UTR, to provide a more comprehensive understanding of its role in post-transcriptional regulation. Employing advanced techniques like CLIP-seq and ribosome profiling to map FMRP's binding sites and functional impacts across the transcriptome will be crucial. Such research will help elucidate the full extent of FMRP's regulatory network and its implications in complex neurodevelopmental disorders like FXS.

Materials and methods

DNA constructs

For luciferase assays, the 5×BoxB FLuc reporters, RLuc plasmid, plasmids expressing λN-HA tagged proteins (dFMRP, AGO1, and GW182), and miR-958 have all been described previously [17,20,33,48]. We constructed the dFMRP deletion plasmids of function domains exactly as described previously [22,23]. To make the 3X and 1X plasmids, we removed the 5XBoxB sequence from the pAc5.1C-FLuc-Stop-5BoxB plasmid (Addgene #21301) between the EcoRI and XhoI sites and replaced it with oligos encoding for the 3×BoxB or 1×BoxB stem loop sequences. The pAc5.1C plasmid contains the *actin5C* promotor for strong expression and the SV40 3'UTR for efficient 3' end formation. The 0×BoxB plasmid was generated by blunting the EcoRI and XhoI sites and then recircularizing the plasmid. For the experiments using dFMRP deletion constructs, we cloned the dFMRP sequences from plasmids we have previously described into pAc5.1C-FLuc-Stop-5BoxB [17]. For S2 cell colocalization experiments, GFP-tagged dFMRP has been previously described [17]. The single isoform of DCR1 was amplified by RT-PCR from mRNA isolated from S2 cells and reverse transcribed using the Oligo(dT)-primed RNA to cDNA EcoDry premix (Takara Bio). The CDS for AGO1 and GW182 were PCR amplified from pAFW-Ago1 (Addgene #50553) and LD47780 (DGRC) respectively. All three were cloned downstream of mCherry in pAc5.1A (Invitrogen). For the co-immunoprecipitation experiments, the pAc5.1-λN-HA:dFMRP and pAFW-AGO1 plasmids have been previously described [17,49]. To construct the FLAG-tagged GW182 plasmid, the CDS for GW182 was PCR amplified from LD47780 (DGRC) and inserted into the pAFW vector (DGRC) by Gateway Cloning (Invitrogen). For the EMSA experiments, the dFMRP CDS was PCR amplified from pAc5.1-EGFP-dFMRP and transferred into pET-His6-MBP-TEV (Addgene #29656) by ligation-independent cloning following QB3 Macrolab protocols (https://qb3.berkeley.edu/facility/qb3-macrolab/). DNA sequences for all oligonucleotides used for PCR throughout this study are provided in Supplementary Table 1.

Cell culture and luciferase assays

Drosophila S2 cells (S2-DRSC; DGRC #181) were maintained at 25°C in 75 cm^2 cell culture-treated flasks in M3 media (Sigma) supplemented with 10% FBS (Gibco). Transfections were carried out in 12-well plates using Effectene transfection reagent (Qiagen). Unless otherwise indicated (for gradient experiments), the transfection mixture (per well) contained 0.05 µg of the FLuc reporter plasmid, 0.2 µg of the RLuc transfection control plasmid and 0.5 µg of the plasmid expressing the λN-HA control, λN-HA-tagged, or untagged proteins. For RNAi experiments, PCR primers containing a 5' binding site for T7 RNA polymerase were designed using SnapDragon (https://www.flyrnai.org/snapdragon) and used to amplify sequences targeting each gene. Sequences were selected that had no predicted off-target binding sites in the fly genome. dsRNA was synthesized from a PCR product using a MEGAscript T7 kit (Ambion). One microgram of dsRNA (per well) was added to each transfection mixture. All transfections were done in triplicate and luciferase activity measured after 3 days using the Dual Luciferase Reporter Assay System (Promega).

Western blotting and quantitative real time PCR (qPCR)

Western blotting was done essentially as previously described [17]. Antibodies targeting dFMRP (dilution 1:1000; Abcam #10299), DCR1 (dilution 1:1000; Abcam #4735), AGO1 (dilution 1:2000; Abcam #5070), GW182 (dilution 1:2000) [50], Armitage (dilution 1:1000) [25], HA (dilution 1:500; Cell Signaling Technology #2367), FLAG (dilution 1:1000; Sigma M2), and β-actin (dilution 1:1000; Abcam #8224). Bound primary antibodies were detected with horseradish peroxidase-coupled secondary antibodies (Cell Signaling Technologies) and then visualized by chemiluminescence (using SuperSignal West Chemiluminescence kits from Thermo Fisher).

Quantification of RNA abundance in S2 cells was done by qPCR. On the day of luciferase assays, total RNA was isolated from the remaining cells using TRIzol (Invitrogen) followed by column purification using the RNeasy Mini Kit (Qiagen) followed by DNAse treatment. One microgram of total RNA was reverse transcribed using the double primed RNA to cDNA EcoDry premix (Takara Bio). Primers were designed targeting FLuc, Rluc, and β-actin as a control and analysed on an IQ5 Thermal Cycler (BioRad) using the iQ SYBR Green Supermix (BioRad). All reactions were done in triplicate. To evaluate the specificity of PCR amplification for each primer set, we performed melt curve analysis. For relative quantification of transcript levels, we used the ΔΔCt method.

Polysome profiling

S2 cells were transfected as described for luciferase assays except plasmid concentrations were doubled for 6-well plates. Three wells were transfected for each set of plasmids. After 3

days, cells were incubated with cycloheximide at a final concentration of 100 µg/ml for 10 min at 25°C. Cells were then pooled (~10 × 10^6 cells total), washed in ice-cold PBS with cycloheximide, and resuspended in polysome lysis buffer (10 mM HEPES (pH 7.4), 10 mM $MgCl_2$, 150 mM KCl, 0.5% NP-40, 0.5 mM DTT, 100 U/ml SUPER-RNAse inhibitor (Thermo Fisher), complete EDTA-free protease inhibitor (Roche), and 100 µg/ml cycloheximide), and then lysed using a dounce homogenizer. Cell debris was removed by centrifugation at 14,000*g* at 4°C. Three hundred microlitre of each supernatant was layered on top of a linear 10–50% sucrose gradient in 10 mM HEPES and 10 mM HEPES (pH 7.4), 15 mM $MgCl_2$, 150 mM KCl). Centrifugation was done using an SV-41 rotor (Beckman) for 2 h 30 min at 37,000 rpm at 4°C. Polysome profiles were measured by absorbance and fractions collected using a Gradient Station and Fractionator (Biocomp). For RNA analysis, 200 µl of each fraction was used. RNA was purified using TRIZOL followed by column purification using the DirectZol RNA mini kit (Zymo Research). Fractions were pooled (proportionally) based on polysome profiles into RNP, 40S ribosome, 60S ribosome, monosome, and polysomes (Supplemental Figure S1). RNA was then reverse transcribed using the double primed RNA to cDNA EcoDry premix (Takara Bio). RNA abundance was determined by qPCR using primers targeting FLuc. Fold enrichment was calculated relative to the RNP sample. For protein analysis, protein was precipitated from 200 µl of each fraction with TCA and pellets solubilized in 100 µl of 2× Laemmli sample buffer for 10 min at 95°C. Fifteen microitre of each sample was loaded onto a 4–20% Mini Protean gel (BioRad), separated, and analysed by Western blot.

Co-immunoprecipitation

S2 cell transfections were carried out in 6-well plates using Effectene transfection reagent (Qiagen). Each well was transfected with 1 µg of the pAc5.1-λN-HA:dFMRP and 1 µg pAFW-AGO1 or pAFW-GW182 plasmids. After incubation at 25°C for 3 days, cells were resuspended in ice-cold Pierce IP Lysis Buffer (25 mM Tris (pH = 7.4), 150 mM NaCl, 1 mM EDTA, 1% NP-40 and 5% glycerol). Cell debris was removed by centrifugation at 13,000*g* for 10 min at 4°C. HA-tagged FMRP (and associated proteins) was immunoprecipitated using the HA-Tag IP/Co-IP kit (Pierce). Protein was dissociated from magnetic beads by incubation with 50 µl of 2× Laemmli sample buffer for 10 min at 95°C and subjected to SDS-PAGE followed by Western analysis.

S2 cell imaging and colocalization

S2 cell transfections were carried out in 6-well plates using Effectene transfection reagent (Qiagen). Each well was transfected with 1 µg of the pAc5.1-EGFP:dFMRP and 1 µg of pAc5.1-mCherry plasmids containing DCR1, AGO1, or GW182. After incubation at 25°C for 3 days, cells were resuspended and 200 µl transferred to poly-D-lysine coated #1.0 glass bottom dishes (Cellvis) and allowed to settle for ~5 min. Live cell fluorescence images were obtained using an Olympus FV3000 scanning confocal microscope with a 100× (N.A. = 1.4) objective digitally zoomed to 2.95 (the optimal setting for this objective per the Fluoview software). To determine the degree of colocalization, single focal planes were obtained for 12 to 14 cells and analysed in FIJI/ImageJ2 using the JACoP plugin [51]. Images were cropped to the smallest area possible to eliminate colocalization outside of the cell of interest. In JACoP, Pearson's and Mander's coefficient results were generated and recorded for statistical analysis.

Protein purification and electrophoretic mobility shift assay

BL21-DE3 cells (New England Biolabs) were transformed with pET-His6-MBP-TEV-dFMRP and protein expression induced by incubation with IPTG. After ~4 hours of expression, cells were lysed in lysis buffer (50 mM Tris (pH = 8), 100 mM NaCl, 5 mM β-mercaptoethanol, 5% glycerol, and 1 mM imidazole). MBP-tagged protein was purified by affinity column chromatography using Ni-IMAC resin (Thermo Fisher) followed by size-exclusion chromatography using a Superdex 200 column (Sigma Aldrich). Protein was eluted off columns and then analysed with SDS-PAGE followed by Coomassie staining (Supplemental Figure S3). The remaining protein was run through a 50 kDA cut off spin concentrator (Millipore) and dialysed into 2X storage buffer (48 mM HEPES, 500 mM NaCl, 20% glycerol, and 4 mM DTT). The sample was further diluted by half with molecular grade 100% glycerol (Sigma Aldrich) and stored at −80°C prior to use.

For EMSA experiments, short RNAs corresponding to the 17 nucleotide BoxB stem loop or the A14 unstructured control (a polymer of 14 adenosines) were synthesized *in vitro* and purified as we have previously described [52]. Single stranded RNA and purified full-length FMRP were mixed and then allowed to bind at room temperature for 20 min. There was 1 µg of RNA added to each binding reaction for both the BoxB (MW = 5805 for 5' OH) and A14 (MW = 4626 for 5' OH). Molar ratios indicated are protein to RNA. After incubation, the samples were separated by electrophoresis on a 20% native polyacrylamide gel. Following electrophoresis, these 'cold' native gels were stained with methylene blue and RNA bands imaged for analysis.

Fly stocks, NMJ dissections, immunofluorescence, and quantification

For all experiments, both male and female flies were used for analysis. All crosses were incubated at 25°C with 12-h light/dark cycles and 60% humidity on standard Bloomington media. Flies used in this study were w^{1118} *(Iso31),* $dFmr1^{\Delta 113}$, $Ago1^{K00208}$ (Bloomington *Drosophila* Stock Center) and gw^{1} [50]. The NMJ dissections were done essentially as previously described [53]. Larval body wall preps were prepared by dissecting wandering 3rd instar larvae in Ca^{2+}-free HL3 saline. For imaging the NMJ, larval preps were fixed with 3.5% paraformaldehyde in PBS and then immunostained with antibodies targeting presynaptic horseradish peroxidase (HRP) and postsynaptic discs large (DLG). The specific antibodies used were Alexa 568-conjugated anti-HRP (1:1000,

Jackson Immunoresearch), mouse anti-DLG (1:100, Developmental Studies Hybridoma Bank), and an anti-mouse Alexa 488-conjugated secondary (1:1000, Molecular Probes). Preps were then mounted on charged slides in DAPI Fluoromount G (Southern Biotech) and images were obtained using an Olympus FV3000 scanning confocal microscope with a 60× (N.A. = 1.42) objective. The number of type 1b synaptic boutons at muscles 6 and 7 (m6/7) in abdominal segment 3 (A3) was manually quantified using the built-in cell counting plugin in FIJI/ImageJ2 as previously described [54]. Boutons were defined as a distinctive swelling at the NMJ marked by both DLG and HRP and distinguished from type 1s boutons based on size and a greater amount of DLG staining. To account for differences between genotypes in the scaling of NMJs to muscle size, synaptic bouton numbers were normalized to muscle surface area (MSA). MSA was calculated from images of the corresponding m6/7 obtained with a 20× objective (N.A. = 0.85) and quantified in FIJI/ImageJ2. Data were collected from 8 to 10 larvae for each of the indicated genotypes for statistical analysis.

Quantification and statistical analysis

All data were recorded in Excel (Microsoft) and then graphed and analysed in Prism (GraphPad). The results were considered statistically significant if $p < 0.05$. Error bars throughout the study are mean ± SEM. n.s. = not significant, $^{*}p < 0.05$, $^{**}p < 0.01$, $^{***}p < 0.001$, and $^{****}p < 0.0001$.

Acknowledgments

We would like to thank members of the Barbee lab for useful discussions. The deadenylation- and scanning-independent reporter plasmids were a kind given by Dr Elisa Izaurralde. Plasmids not developed for use in this study were obtained from Addgene and the *Drosophila* Genomics Resource Center. S2-DRSC cells were purchased from the *Drosophila* Genomics Resource Center. The *dFmr1* and *Ago1* fly lines were obtained from the Bloomington *Drosophila* Stock Center. The *GW182* fly line and antibody were a generous gift from Andrew Simmonds. Finally, the Armitage antibody was a gift from Peng Jin.

Disclosure statement

No potential conflict of interest was reported by the author(s).

Funding

This work was supported by a National Institutes of Health [R15MH114019] award to SAB.

Data availability statement

The authors confirm that the data supporting the findings of this study are available within the article and its supplementary material.

References

[1] Santoro MR, Bray SM, Warren ST. Molecular mechanisms of fragile X syndrome: a twenty-year perspective. Annu Rev Pathol. 2012;7:219–245.
[2] Richter JD, Zhao X. The molecular biology of FMRP: new insights into fragile X syndrome. Nat Rev Neurosci. 2021 Apr;22(4):209–222.
[3] Lai A, Valdez-Sinon AN, Bassell GJ. Regulation of RNA granules by FMRP and implications for neurological diseases. Traffic. 2020 Jul;21(7):454–462.
[4] Chen E, Joseph S. Fragile X mental retardation protein: a paradigm for translational control by RNA-binding proteins. Biochimie. 2015 Jul;114:147–154.
[5] Darnell JC, Klann E. The translation of translational control by FMRP: therapeutic targets for FXS. Nat Neurosci. 2013 Nov;16(11):1530–1536.
[6] De Rubeis S, Pasciuto E, Li KW, et al. CYFIP1 coordinates mRNA translation and cytoskeleton remodeling to ensure proper dendritic spine formation. Neuron. [2013 Sep 18];79(6):1169–1182.
[7] Feng Y, Absher D, Eberhart DE, et al. FMRP associates with polyribosomes as an mRNP, and the I304N mutation of severe fragile X syndrome abolishes this association. Mol Cell. 1997 Dec;1(1):109–118.
[8] Athar YM, Joseph S. The human fragile X mental retardation protein inhibits the elongation step of translation through its RGG and C-terminal domains. Biochemistry. [2020 Oct 13];59(40):3813–3822.
[9] Chen E, Sharma MR, Shi X, et al. Fragile X mental retardation protein regulates translation by binding directly to the ribosome. Mol Cell. [2014 May 8];54(3):407–417.
[10] Kenny P, Ceman S. RNA secondary structure modulates FMRP's Bi-functional role in the MicroRNA pathway. Int J Mol Sci. 2016 Jun;17(6):985.
[11] Cheever A, Ceman S. Phosphorylation of FMRP inhibits association with dicer. RNA. 2009 Mar;15(3):362–366.
[12] Jin P, Zarnescu DC, Ceman S, et al. Biochemical and genetic interaction between the fragile X mental retardation protein and the microRNA pathway. Nat Neurosci. 2004 Feb;7(2):113–117. doi: 10.1038/nn1174
[13] Lee EK, Kim HH, Kuwano Y, et al. hnRNP C promotes APP translation by competing with FMRP for APP mRNA recruitment to P bodies. Nat Struct Mol Biol. 2010 Jun;17(6):732–739.
[14] Kenny PJ, Zhou HJ, Kim M, et al. MOV10 and FMRP regulate AGO2 association with MicroRNA recognition elements. Cell Rep. [2014 Dec 11];9(5):1729–1741. doi: 10.1016/j.celrep.2014.10.054
[15] Kenny PJ, Kim M, Skariah G, et al. The FMRP-MOV10 complex: a translational regulatory switch modulated by G-Quadruplexes. Nucleic Acids Res. [2020 Jan 24];48(2):862–878.
[16] Niaz S, Hussain MU. Role of GW182 protein in the cell. Int J Biochem Cell Biol. 2018 Aug;101:29–38.
[17] Starke EL, Zius K, Barbee SA. FXS causing missense mutations disrupt FMRP granule formation, dynamics, and function. PLOS Genet. 2022 Feb;18(2):e1010084.
[18] Fukaya T, Iwakawa HO, Tomari Y. MicroRNAs block assembly of eIF4F translation initiation complex in Drosophila. Mol Cell. [2014 Oct 2];56(1):67–78.
[19] Ding XC, Grosshans H. Repression of microRNA targets at the initiation level of translation requires GW182 proteins. Embo J. [2009 Feb 4];28(3):213–222.
[20] Zekri L, Kuzuoglu-Ozturk D, Izaurralde E. GW182 proteins cause PABP dissociation from silenced miRNA targets in the absence of deadenylation. Embo J. [2013 Apr 3];32(7):1052–1065. doi: 10.1038/emboj.2013.44
[21] Kuzuoglu-Ozturk D, Bhandari D, Huntzinger E, et al. miRISC and the CCR4-NOT complex silence mRNA targets independently of 43S ribosomal scanning. Embo J. [2016 Jun 1];35(11):1186–1203.
[22] Gareau C, Houssin E, Martel D, et al. Characterization of fragile X mental retardation protein recruitment and dynamics in drosophila stress granules. PLOS ONE. 2013;8(2):e55342.
[23] Gareau C, Martel D, Coudert L, et al. Characterization of fragile X mental retardation protein granules formation and dynamics in Drosophila. Biol Open. [2013 Jan 15];2(1):68–81.
[24] Zhou Y, Hu Y, Sun Q, et al. Non-coding RNA in fragile X syndrome and converging mechanisms shared by related disorders. Front Genet. [2019 Mar 1];10:139.

[25] Huang HD, Li YJ, Szulwach KE, et al. AGO3 slicer activity regulates mitochondria-nuage localization of Armitage and piRNA amplification. J Cell Biol. [2014 Jul 21];206(2):217–230.
[26] Elkayam E, Faehnle CR, Morales M, et al. Multivalent recruitment of human argonaute by GW182. Mol Cell. [2017 Aug 17];67 (4):646–658 e3.
[27] Jonas S, Izaurralde E. Towards a molecular understanding of microRNA-mediated gene silencing. Nat Rev Genet. 2015 Jul;16 (7):421–433.
[28] Ramos A, Hollingworth D, Pastore A. G-quartet-dependent recognition between the FMRP RGG box and RNA. RNA. 2003 Oct;9(10):1198–1207.
[29] Darnell JC, Fraser CE, Mostovetsky O, et al. Kissing complex RNAs mediate interaction between the fragile-X mental retardation protein KH2 domain and brain polyribosomes. Gene Dev. [2005 Apr 15];19(8):903–918.
[30] Ascano M Jr., Mukherjee N, Bandaru P, et al. FMRP targets distinct mRNA sequence elements to regulate protein expression. Nature. [2012 Dec 20];492(7429):382–386.
[31] Bechara EG, Didiot MC, Melko M, et al. A novel function for fragile X mental retardation protein in translational activation. PLOS Biol. 2009 Jan;7(1):133–145.
[32] Tsang B, Arsenault J, Vernon RM, et al. Phosphoregulated FMRP phase separation models activity-dependent translation through bidirectional control of mRNA granule formation. Proc Natl Acad Sci USA. [2019 Mar 5];116(10):4218–4227.
[33] Nesler KR, Sand RI, Symmes BA, et al. The miRNA pathway controls rapid changes in activity-dependent synaptic structure at the drosophila melanogaster neuromuscular junction. PLOS ONE. 2013;8(7):e68385.
[34] Zhang YQ, Bailey AM, Matthies HJ, et al. Drosophila fragile X-related gene regulates the MAP1B homolog futsch to control synaptic structure and function. Cell. [2001 Nov 30];107(5):591–603.
[35] Schuster CM. Glutamatergic synapses of drosophila neuromuscular junctions: a high-resolution model for the analysis of experience-dependent potentiation. Cell Tissue Res. 2006 Nov;326(2):287–299.
[36] Collins CA, DiAntonio A. Synaptic development: insights from Drosophila. Curr Opin Neurobiol. 2007 Feb;17(1):35–42.
[37] Rohrbough J, Grotewiel MS, Davis RL, et al. Integrin-mediated regulation of synaptic morphology, transmission, and plasticity. J Neurosci. [2000 Sep 15];20(18):6868–6878. doi: 10.1523/JNEUROSCI.20-18-06868.2000
[38] Lahey T, Gorczyca M, Jia XX, et al. The drosophila tumor suppressor gene dlg is required for normal synaptic bouton structure. Neuron. 1994 Oct;13(4):823–835.
[39] Napoli I, Mercaldo V, Boyl PP, et al. The fragile X syndrome protein represses activity-dependent translation through CYFIP1, a new 4E-BP. Cell. [2008 Sep 19];134(6):1042–1054.
[40] Darnell JC, Van Driesche SJ, Zhang C, et al. FMRP stalls ribosomal translocation on mRNAs linked to synaptic function and autism. Cell. [2011 Jul 22];146(2):247–261.
[41] Miyoshi K, Okada TN, Siomi H, et al. Characterization of the miRNA-risc loading complex and miRNA-risc formed in the drosophila miRNA pathway. RNA. 2009 Jul;15(7):1282–1291.
[42] Fabian MR, Mathonnet G, Sundermeier T, et al. Mammalian miRNA RISC recruits CAF1 and PABP to affect PABP-Dependent deadenylation. Mol Cell. [2009 Sep 24];35 (6):868–880.
[43] Zekri L, Huntzinger E, Heimstadt S, et al. The silencing domain of GW182 interacts with PABPC1 to promote translational repression and degradation of MicroRNA targets and is required for target release. Mol Cell Biol. [2009 Dec 1];29 (23):6220–6231.
[44] Zalfa F, Adinolfi S, Napoli I, et al. Fragile X mental retardation protein (FMRP) binds specifically to the brain cytoplasmic RNAs BC1/BC200 via a novel RNA-binding motif. J Biol Chem. [2005 Sep 30];280(39):33403–33410.
[45] Darnell JC, Jensen KB, Jin P, et al. Fragile X mental retardation protein targets G quartet mRNAs important for neuronal function. Cell. [2001 Nov 16];107(4):489–499.
[46] Schaeffer C, Bardoni B, Mandel JL, et al. The fragile X mental retardation protein binds specifically to its mRNA via a purine quartet motif. Embo J. [2001 Sep 3];20(17):4803–4813.
[47] Darnell JC, Fraser CE, Mostovetsky O, et al. Discrimination of common and unique RNA-binding activities among fragile X mental retardation protein paralogs. Hum Mol Genet. [2009 Sep 1];18(17):3164–3177.
[48] Eulalio A, Huntzinger E, Izaurralde E. GW182 interaction with argonaute is essential for miRNA-mediated translational repression and mRNA decay. Nat Struct Mol Biol. 2008 Apr;15 (4):346–353.
[49] Kawamata T, Seitz H, Tomari Y. Structural determinants of miRNAs for RISC loading and slicer-independent unwinding. Nat Struct Mol Biol. 2009 Sep;16(9):953–U77.
[50] Schneider MD, Najand N, Chaker S, et al. Gawky is a component of cytoplasmic mRNA processing bodies required for early drosophila development. J Cell Biol. [2006 Jul 31];174 (3):349–358.
[51] Bolte S, Cordelieres FP. A guided tour into subcellular colocalization analysis in light microscopy. J Microsc. 2006 Dec;224(Pt 3):213–232. doi: 10.1111/j.1365-2818.2006.01706.x
[52] Langeberg CJ, Welch WRW, McGuire JV, et al. Biochemical characterization of yeast Xrn1. Biochemistry. [2020 Apr 21];59 (15):1493–1507.
[53] Patel PH, Wilkinson EC, Starke EL, et al. Vps54 regulates drosophila neuromuscular junction development and interacts genetically with Rab7 to control composition of the postsynaptic density. Biol Open. [2020 Aug 25];9(8). doi: 10.1242/bio.053421
[54] Pradhan SJ, Nesler KR, Rosen SF, et al. The conserved P body component HPat/Pat1 negatively regulates synaptic terminal growth at the larval drosophila neuromuscular junction. J Cell Sci. [2012 Dec 15];125(Pt 24):6105–6116.